

Retinotopically organized left to right hemisphere functional connectivity in human V1 using high-resolution fMRI at 7T

J. R. Polimeni¹, K. Fujimoto¹, B. Fischl^{1,2}, D. N. Greve¹, and L. L. Wald^{1,3}

¹Athinoula A. Martinos Center for Biomedical Imaging, Department of Radiology, Harvard Medical School, Massachusetts General Hospital, Charlestown, MA, United States, ²Computer Science and AI Lab (CSAIL), Massachusetts Institute of Technology, Cambridge, MA, United States, ³Harvard-MIT Division of Health Sciences and Technology, Massachusetts Institute of Technology, Cambridge, MA, United States

Introduction: Functional connectivity analysis of resting-state fMRI data has been used to investigate large-scale networks of brain activity [1] and reflects connections between visual cortical areas [2,3] that have known direct anatomical connections in non-human primates [4]. In addition to direct anatomical connections, rs-fMRI detects correlations from areas connected by polysynaptic or common-drive associations. For example, left to right hemisphere V1 correlations are often observed in human primary visual cortex (V1) [2,3], despite the lack of callosal connections in human V1 [5]. Here we utilize these common-mode correlations to investigate whether functional connectivity analysis exhibits sufficient tangential spatial specificity to detect retinotopic organization of the cross-hemispheric correlations. We generate four topographically-corresponding ROIs in the left and right V1 and assess the 4×4 across-hemisphere correlation matrix. Not only are strong inter-hemispheric correlations apparent in the data, but the pattern of functional connectivity follows the retinotopic layout—presumably due to the retinotopically organized common drive from LGN. This indicates that despite the indirect nature of these inter-hemispheric connections, an orderly topographic pattern is present and functional connectivity analysis possesses the specificity to detect small-scale organization of the connections within a single cortical area.

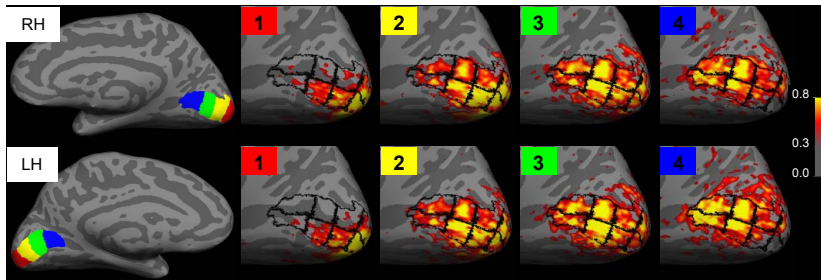


Fig. 1: (Left) Four color-coded retinotopically corresponding seeds in each hemisphere. (Right, top row) Correlation maps in the right hemisphere from ipsilateral seeds in right hemisphere (Right, bottom row) correlations in right hemisphere from left hemisphere seeds.

Methods: Two healthy subjects were studied with a 7T Siemens scanner equipped with AC84 head gradients (80 mT/m, 400 T/m/s) and a custom-built 32-channel receive array. The BOLD acquisition consisted of 1mm isotropic resolution GE single-shot EPI with 64 oblique-transverse slices parallel to the calcarine sulcus, 1.0-mm thick, no slice gap with TR/TE/flip=4000ms/34ms/90°, FOV=192mm×192mm, 192×192 matrix, bandwidth=1502 Hz/pixel, R=3 GRAPPA acceleration yielding an effective echo-spacing of 0.27 ms. Four 5 min 20 sec scans were acquired in each session with eyes-open fixation.

The position of V1 was predicted in each subject offline with a surface-based atlas [6]. The resting-state data was corrected for slice timing, motion corrected, then temporally low-pass filtered with a cutoff of 0.08 Hz. Average signals from the whole brain, ventricles, and white matter along with the motion parameters were regressed out of the time series data [7]. For each subject, surface reconstructions of the inner and outer boundaries of the cortical gray matter were generated by FREESURFER from 1 mm MPRAGE data collected in a separate 3T scan session. Nine additional intermediate surfaces were determined as a function of cortical depth. The functional volumes were accurately aligned to the surfaces with a boundary-based registration method [8]. The voxels intersecting the pial surface layer were excluded from the analysis due to the previously observed degraded point-spread function seen at the pial surface [9]. For each subject, V1 was divided into four roughly equal-sized ROIs on the surface of each hemisphere, and the ROI was used in a seed-based functional connectivity analysis. V1 correlation maps were computed with both contralateral and ipsilateral seeds and the correlations between every combination of the four retinotopically organized ROIs formed a 4×4 correlation matrix.

Results: Area V1 exhibited strong cross-hemispheric correlations in each subject. Fig. 1 compares the correlation maps calculated from contralateral and ipsilateral seeds for each retinotopic ROI. The correlation maps generated from ipsilateral and contralateral seeds in retinotopically-corresponding locations exhibited a strong resemblance and the center of the high-correlation region follows the position of the ROI. The difference in correlations between retinotopically corresponding ROIs and non-corresponding ROIs was statistically significant for each ROI investigated, suggesting that the overall correlation pattern between V1 in the left and right hemisphere was retinotopically structured. The retinotopic organization leads to a diagonal-dominant structure in the 4×4 correlation matrix (Fig. 4).

Discussion: Retinotopic anatomical connections have been observed between several visual areas in non-human primates [4,10], yet the presence of strong cross-hemispheric correlations given the lack of callosal connections in human [5] indicates that the common input stage also possesses retinotopic organization, likely stemming from feedforward signals from the retina relayed by the LGN. The observation of retinotopic correlations demonstrates that rsMRI has sufficient specificity for studying the organization of functional connectivity within individual cortical areas.

References: [1] Biswal *et al.* (1995) *MRM* 34:537-41. [2] Lowe *et al.* (1998) *NeuroImage* 7:119-32. [3] Tian *et al.* (2007) *NeuroImage* 36:684-90. [4] Felleman & Van Essen (1991) *Cereb Cortex* 1:1-47. [5] Clarke & Miklossy (1990) *J Comp Neurol* 298:188-214. [6] Hinds *et al.* (2009) *NeuroImage* 46:915-22. [7] Van Dijk *et al.* (2008) *Soc Neurosci Abs* 885.24. [8] Greve & Fischl (2009) *NeuroImage* 48:63-72. [9] Polimeni *et al.* (2009) *Proc ISMRM* 1559. [10] Weller & Kaas (1983) *J Comp Neurol* 220:253-97. **Acknowledgements:** Supported by NCRR P41RR14075 and NIBIB R01EB006847.

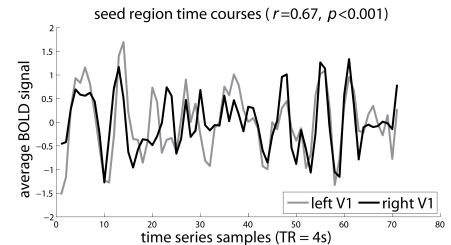


Fig. 2: Two example time courses of retinotopically corresponding ROIs from left and right hemispheres.

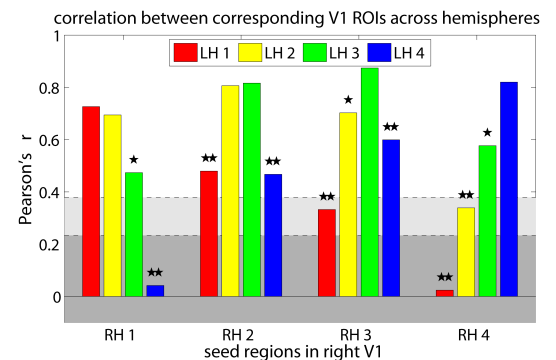


Fig. 3: Correlation between seeds ROIs along four eccentricities. Each bar represents the correlation between a seed in the right hemisphere and a seed in the left. (The dark gray region indicates correlations with $p<0.05$, light gray indicates correlations with $p<0.001$.) A z -test between the correlation of corresponding ROIs with the correlations with the remaining three ROIs was computed; significant differences are marked with one star, highly significant differences with two stars.

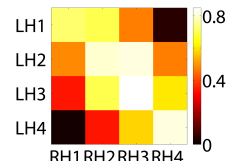


Fig. 4: Corresponding correlation matrix for each region in LH to each region in RH.